Available online at www.sciencedirect.com

SciVerse ScienceDirect

Journal of the European Ceramic Society 32 (2012) 2843–2852

www.elsevier.com/locate/jeurceramsoc

Post-treated incinerator bottom ash as alternative raw material for ceramic manufacturing

L.M. Schabbach [a], F. Andreola [a,*], L. Barbieri [a], I. Lancellotti [a], E. Karamanova [b], B. Ranguelov [b], A. Karamanov [b]

[a] *Department of Materials and Environmental Engineering, University of Modena and Reggio Emilia, Via Vignolese 905, 41100 Modena, Italy*
[b] *Institute of Physical Chemistry, Bulgarian Academy of Sciences, G. Bonchev Str. Block 11, 1113 Sofia, Bulgaria*

Available online 20 February 2012

Abstract

New ceramics based on 60 wt% of alternative raw material derived from post-treated municipal solid waste incinerator bottom ashes and 40 wt% of refractory clay were studied. The chemical analysis of the compositions was evaluated by ICP. The thermal and densification behavior of the ceramic batches were evaluated by DTA-TG and dilatometry techniques, respectively. After that, the degree of sintering at different temperatures and soaking times was evaluated in detail, measuring open and closed porosities, linear shrinkage and water absorption. The crystallinity at different temperatures (during heating and after cooling) and microstructure of the obtained samples were evaluated by high-temperature X-ray diffraction (HTXRD) and scanning electron microscopy (SEM), respectively. For these new ceramics, the experimental results highlighted sintering range between 1190–1240 °C. In addition, the specimens demonstrated low water absorption and high crystallinity (with anorthite as main crystalline phase), leading to mechanical characteristics comparable to those of commercial ceramic products (bending strength > 40 MPa).

Keywords: A. Sintering; B. Microstructure; C. Thermal and mechanical properties; D. Traditional ceramics

1. Introduction

The world production of building and tiles ceramics requires massive amount of natural raw materials, which until now is based mainly on the traditional system clay-silica-feldspar. Nevertheless, several studies made in the last decades are related to the substitution of conventional raw materials by other natural resources as zeolites,[1] volcanic rocks[2,3] and nepheline syenite.[4] Another widely studied possibility is the application of different industrial residues or wastes as alternative raw materials. Many of these works are focused on characterization and utilization of different alternative fluxing agents; this is a consequence of the high cost of feldspars and the limited number of appropriate deposits. Promising results were obtained using soda–lime glass cullet,[5] cathode ray tube of TV or PC monitors (CRT glass)[6] and granite cutting sludge.[7]

Since the new fluxes have different chemical compositions, some of the new ceramic batches show significant variations in the forming and firing behavior. In general, the alternative fluxes form melts with lower viscosity than the corresponding feldspar melts, which decreases the sintering temperature and/or leads to formation of high percentage of glassy phase.[8]

For this reason, in order to obtain sintering behavior and mechanical characteristics similar to the industrial compositions, the feldspars are partially substituted. In general, the addition of higher amount of fluxes leads to an increase of amorphous phase in the final product.

However, if the alternative flux is characterized by a high crystallization trend, the crystallinity of final ceramics might be increased. This effect can be obtained using glass–ceramic frits or waste residues with high crystallization tendency (as slag and fly ashes).[9–11] In this case, due to re-crystallization processes during the sintering and cooling steps, the amount of residual amorphous phase decreases, leading to an improvement of the mechanical properties.[12] Among these residues, the pre-treated bottom ash from municipal solid waste incineration (MSWI) can be selected for testing the feasibility as component into ceramics body.

* Corresponding author at: Dipartimento di Ingegneria dei Materiali e dell'Ambiente, Università degli Studi di Modena e Reggio Emilia, Via Vignolese 905, 41100 Modena, Italy. Tel.: +39 059 2056237; fax: +39 059 2056243.
E-mail address: andreola.fernanda@unimore.it (F. Andreola).

0955-2219/$ – see front matter © 2012 Elsevier Ltd. All rights reserved.
doi:10.1016/j.jeurceramsoc.2012.01.020

In 2008 about 32.5 millions tons of municipal solid wastes (MSW) have been produced in Italy. Great amounts (44.9%) have been landfilled without pre-treatment, while only 10.9% of the MSW have been incinerated.[13] From the incineration of municipal waste, bottom ash with volume ranged between 10% and 12% of the starting waste volume and weight between 20% and 35% of the starting waste weight, is obtained.[14,15] According to these data, in Italy, the annual production of MSWI bottom ash could be estimated in about 797 thousand tons, a significant amount of which is landfilled (about 49.2%).[16] Although bottom ash is classified as non-hazardous waste according to the European Waste Catalog (190101), its disposal requires high costs. Therefore, the development of reusing incineration bottom ash as ceramic material has to be strongly promoted.[17] This idea has a double environmental benefit: avoidance of MSWI ashes disposal and reduction of ceramic raw materials use.In the last years in Italy some companies became active and specialized in post-treatment technologies of bottom ashes. The objective is minimizing waste production by transforming it in a reusable material. The treatment starts from a complex process of selection and physical/mechanical treatment (aging, sieving and washing) of incineration bottom ashes. After the process, an inert material with silica-based matrix, rich in iron, calcium and aluminum oxides is obtained. This material can be successfully applied mainly in cement as substitute of extracted raw materials or in the ceramic sector.[18–20]

Ceramic bodies, such as tiles, are heterogeneous materials, consisting mainly of natural raw materials with wide range of composition.[21] For this reason, such bodies could tolerate different types of alternative raw materials, even in high percentages. This is achieved by the reduction in the use of raw materials, transport, energy consumption, waste processing and by recycling of high-quality secondary raw materials.

Porcelain stoneware tile, characterized by very low water absorption (<0.5)[21] and high values of density and mechanical properties (bending strength >35 MPa), represents the best product, in terms of technical performances, developed in the field of ceramic tiles belonging to BIa group. This product is the result of an industrial processing of a mix of raw materials, rich in fluxing agents that, fired at temperature around 1200 °C, develops a large amount of glassy phase (60–70%) able to obtain a strongly densified material. A typical composition contains 25–50% of kaolinitic and ball clays, 50–60% of feldspar sand and 5–10% of quartz sand.

Single firing porous tile is characterized by relatively high water absorption (>6%),[21] in comparison to porcelain stoneware. It is a product with both low density and mechanical properties (bending strength >22 MPa). It is a useful product suitable for wall covering, resulting from an industrial processing of a mix of raw materials with low added value (BIIa group). A typical composition contains 30–40% of ball clays, 20–50% of feldspar sand and 10–15% of carbonate.The relatively high firing temperature, normally adopted (>1000 °C) in the tiles production, should promote effective incorporation of wastes into ceramic matrix. Moreover, strongly reactive heavy metals and transitions metals, often contained in post treated bottom ash (PTBA), tend to promote sintering process. The incorporation of the PTBA in ceramic body mixes can have a positive effect on the firing process, by saving energy as a consequence of the reduction of sintering temperature. In addition, the final products usually do not show hazardous leaching characteristics.[22–24]

In the present work the authors have focused their attention on the obtainment of new ceramics based on huge amount (60 wt%) of alternative raw material derived from post-treated municipal solid waste incinerator and 40 wt% of refractory clay. The new ceramics were tailored to replace feldspar and quartz sand completely. The end products obtained were characterized in accordance of ISO rules in order to define their UNI EN ISO classification. Besides, to evaluate their safety for real applications, leaching test were conducted following UNI EN 12457-2.

Table 1
Chemical compositions of PTBA and K components (oxide wt%) and calculated batch of CLK and CFK.

OXIDE	PTBA (F)	PTBA (L)	K	CFK	CLK
SiO_2	30.31	47.40	47.1	37.03	47.28
Al_2O_3	13.33	9.95	36.1	22.44	20.41
Fe_2O_3	10.82	4.38	0.75	6.79	2.93
CaO	20.75	18.80	0.40	12.61	11.44
MgO	2.83	2.91	0.27	1.81	1.85
Na_2O	1.94	4.53	0.59	1.40	2.95
K_2O	0.94	0.98	1.06	0.99	1.01
TiO_2	1.07	0.75	0.24	0.74	0.55
B_2O_3	0.30	0.56	–	0.18	0.34
MnO	0.18	0.11	–	0.11	0.07
ZnO	0.83	0.34	–	0.50	0.20
PbO	0.36	0.31	–	0.22	0.19
SO_3	1.74	1.01	–	1.04	0.61
P_2O_5	1.96	1.26	–	1.18	0.76
CuO	0.68	0.47	–	0.41	0.28
Cloride	0.48	–	–	0.29	0.02
Others	0.10	0.20	–	0.06	0.12
L.o.I	11.7	5.58	12.49	12.02	8.34
Total	100.40	99.54	99.00	99.84	99.33

2. Experimental procedure

2.1. Materials

In this study a post-treated bottom ash (PTBA) derived from municipal incinerator was chosen. Two fractions of the waste: F: fine (0–2 mm) and L: coarse (2–8 mm) were used together with a refractory clay: K kaolin ceramic grade (Balco, Italy).

2.2. Mixtures preparation

Two ceramic batches, containing 60 wt% of PTBA (F and L fractions) and 40 wt% of a refractory clay were prepared. The results of the chemical analysis (determined by Inductively Coupled Plasma, ICP, Varian Liberty 200) of raw materials (in oxides wt%) and the calculated batches CFK (PTBA fine fraction/kaolin) and CLK (PTBA large fraction/kaolin) are reported in Table 1.

In order to prepare suitable press-powder, the raw materials were ground and sieved below 75 μm. Each batch composition was prepared by dry-grinding, humidified with 6 wt% of distilled water, and finally the green samples were pressed at 40 MPa. Bar samples (50 mm × 5 mm × 4 mm) were sintered in an electric laboratory furnace (Nambertherm) at 10 °C/min heating and 1 h soaking step at different temperatures (1100–1240 °C range). Moreover, parallelepiped samples (100 mm × 50 mm × 8 mm) were uniaxial pressed at 40 MPa and the obtained specimens (semi-industrial samples) were used for bending strength (B.S.) and other technological measurements. These CFK and CLK samples have been dried overnight at 110 °C and then fired in an electric kiln, using 10 °C/min heating rate up to 1210 and 1190 °C, respectively, and with soaking time at the maximum temperature of 1 h.

2.3. Characterization of samples

The sintering process of the mixtures in the temperature range of 20–1300 °C was studied with a horizontal optical dilatometer (Expert System Solutions, Misura HSML ODLT 1400) using heating rate of 20 °C/min, while the thermal behavior (TG/DTA) using the same heating rate was determined by differential thermal analyzer (Netzsch STA 409).

The apparent, ρ_a, skeleton, ρ_s, and absolute, ρ_{as}, densities of the sintered samples were determined and the results were used to evaluate total P_T, closed P_C, and open P_O porosity:

$$P_T = 100 \times \frac{\rho_{as} - \rho_a}{\rho_{as}} \quad (1)$$

$$P_C = 100 \times \frac{\rho_{as} - \rho_s}{\rho_{as}} \quad (2)$$

$$P_O = 100 \times \frac{\rho_s - \rho_a}{\rho_{as}} \quad (3)$$

ρ_a was estimated by an Envelope Density Analyzer (GeoPyc 1360, Micromeritics) using a dry-flow medium, while ρ_s and ρ_{as} by gas (Ar) pycnometer (AccyPy1330, Micromeritic) before and after crashing and milling the samples below 26 μm, respectively.

Detailed porosity measurements were performed by mercury porosimetry technique using (Micromeritics, model Autopore 1215-II) on dried sample pieces (4–5 mm). The samples were put in a penetrometer with 15 mL sample cup and steam volume of 0.38 mL. The pieces were exposed to a vacuum to remove air and vapors in their pores for 10 min. Porosity was evaluated using the set-time equilibrium (10 s) mode between pressure limits of 3.4 kPa and 414 MPa.

For the semi-industrial fired samples, measurements of linear shrinkage (LS%) and water absorption (WA%) according to ISO 10545-3 were performed. Young's modulus (E), shear modulus (G) in GPa and Poisson's ratio (ν) were determined by a Lemmens Grindosonic Electronika MK5 Ltd. instrument using a non-destructive technique. The elastic moduli values were calculated using dimensions, shape and weight data of samples by means of EMOD software program. This test follows the ASTM 1259 method for dynamic elastic modulus.[25]

The bending strength was determined using a flexometer (Nannetti, model CCR) by a three-point loading test with a spam of 80 mm according to UNI EN ISO 10545.4 as the average of five specimens.

The thermal expansion coefficients (α) were determined in the temperature range 25–400 °C using 5 °C/min heating rate by a mechanical horizontal dilatometer (Netzsch, model 402 EP) on bars shaped samples (45 mm × 5 mm × 4 mm).

A qualitative mineralogical study of the materials and final samples was carried out by using a conventional Bragg–Brentano powder diffractometer (X'Pert PRO, Panalytical) with Ni-filtered Cu Kα radiation using bracket holder. The patterns have been recorded on the powdered samples (<38 μm in size) in the 5–70° 2θ range (step size 0.02° and 1 s counting time for each step).

Moreover, to analyze the formation of crystalline phases as a function of the temperature, high-temperature X-ray diffractometer (HTXRD) with a heating chamber (HTK 16) was used. Powders of mixtures (<38 μm) were heated on platinum bar from room temperature to different temperatures (800, 950, 1000 and 1200 °C for the CFK mixture and 800, 950, 1050 and 1200 °C for the CLK mixture, respectively) at which the XRD scanning was performed. The temperatures were chosen on the basis of DTA results (-exo and -endo peaks).

In order to reproduce the industrial cycles a heating rate of 50 °C/min was used and the patterns were collected also during cooling cycle at 950 and 25 °C to control the effect of cooling on the crystallinity. The X-ray diffraction patterns at each temperature were obtained over a range of diffraction 10–70° 2θ, with time per step equal to 25 s. The identification of crystalline phases was made by comparing with data on the JCPDS file.[26]

The microstructure and crystal morphology of the fired samples were observed by scanning electron microscopy (JEOL JSM 6390) coupled with an energy dispersion spectroscopy equipment (INCA X-stream OXFORD).

The environmental impact of the new ceramics was determined by leaching test following the European rule (UNI EN 12457-2: "Compliance test for leaching of granular waste materials and sludge").[27] This method is one stage batch test (the preparation procedure follows the UNI 10802) with liquid to solid ratio of 10:1 kg for materials with particle size below 4 mm, in deionised water for a period of 24 h at room temperature. Solid residue was separated by vacuum filtration through a membrane filter 0.45 μm; on each eluate pH (Digital pHmeter mod. PH6, XS/Eutech) and specific conductivity (Digital conductimeter mod. COND6, XS/Eutech) were determined and after acidification (pH = 2 using HNO_3 65%) metals content was analyzed by ICP/AES. The anions were determined by optical spectrometry (NANOCOLOR 400D). The elements searched were those indicated in the Italian regulation used to identify granulated and monolithic residues for recovering (Decree No. 186, 05/04/2006, All.3).

3. Results and discussion

As observed in Table 1 the inert PTBA contains iron, calcium, aluminum and silicon oxides (in different amount

Table 2
Mineralogy of kaolin and PTBA used in the mixtures.

Materials	Crystalline phases (ICDD)
Kaolin	Quartz, SiO_2 [01–085–0457] Kaolinite, Al_2 (Si_2O_5) $(OH)_4$ [01–078–1996] Illite, (K,H_3O) $Al_2Si_3AlO_{10}$ $(OH)_2$ [026–0911]
PTBA (F fraction)	Quartz, SiO_2 [01–085–0794] Calcite, $CaCO_3$ [024–0027] Akermanite, $(Ca_{1.53}Na_{0.51})(Mg_{0.39}Al_{0.41}Fe_{0.16})Si_2O_7$ [01–072–2127] Albite calcian ordered, (Na,Ca) Al (Si, $Al)_3O_8$ [041–1480]
PTBA (L fraction)	Quartz, SiO_2 [01–085–0794] Calcite, $CaCO_3$ [024–0027] Akermanite-Gehlenite, $Ca_2(Mg_{0.5}Al_{0.5})(Si_{1.5}Al_{0.5}O_7)$ [01–079–2423] Albite calcian ordered, (Na,Ca) Al (Si, $Al)_3O_8$ [041–1480] Covellite, CuS [03–065–3928]

depending on particle size and with major concentration of the heavy metals into the fine fraction) while kaolin clay contains silicon and aluminum oxides. Crystalline phases of the PTBA and kaolin identified by XRD are reported in Table 2. As observed in the kaolin are present kaolinite (Al_2 (Si_2O_5) $(OH)_4$), quartz (SiO_2) and illite ((K,H_3O) $Al_2Si_3AlO_{10}$ $(OH)_2$). Regarding the bottom ash, the L fraction presented as crystalline phases calcite ($CaCO_3$), akermanite-gehlenite ($Ca_2(Mg_{0.5}Al_{0.5})(Si_{1.5}Al_{0.5}O_7)$), quartz ($SiO_2$), albite calcian ordered ($(Na,Ca)Al(Si,Al)_3O_8$) and covellite (CuS) traces; while for the F fraction only calcite, akermanite ($(Ca_{1.53}Na_{0.51})(Mg_{0.39}Al_{0.41}Fe_{0.16})Si_2O_7$), quartz and albite calcian ordered were identified.

The batch chemical compositions (CLK and CFK), reported in Table 1, are completely different with respect to the traditional ceramic products. The significantly low SiO_2 amount and the high percentages of calcium, magnesium and iron oxides make these batches compositions comparable to those of glass–ceramics obtained from industrial wastes.[28]

3.1. Sintering and phase formation

Figs. 1 and 2 show the DTA–TG and dilatometric plots (left scale) of CFK and CLK, respectively, obtained at heating rate of 20 °C/min. At lower temperatures the DTA traces highlight different behavior of CFK and CLK batches, which can be related to differences in their compositions. Due to a higher percentage of organic matter, the exothermic peaks in the range 300–450 °C and the related weight losses (dashed lines) are more intense in CFK confirming the high L.O.I., as well as the endotherm nearly 700 °C due to the $CaCO_3$ decomposition. The DTA and TG effects related to kaolinite deoxydrilation are identical for the two compositions.

The sintering curves (right scale) elucidate that only the kaolinite deoxydrilation at 530 °C leads to linear shrinkage (at about 0.5%). This means that the burning of organic residues and

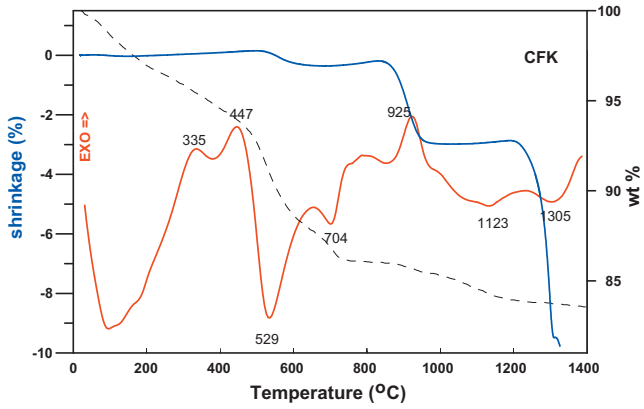

Fig. 1. DTA/TG and DIL curves of CFK composition.

the decarbonization process can increase the porosity of samples. Obviously, this porosity rise must be more evident in CFK composition.

In the range 850–950 °C about 2.5% shrinkage is observed in the both ceramics. These variations correspond to the exo-effects from the DTA curves (with peaks at 925 and 950 °C for CLK and CFK respectively). These effects can be explained by reactions of meta-kaolinite with oxides derived from the alternative raw material to form calcium alluminosilicates.

The DTA traces show that melting of some of the formed crystalline phases is observed in the interval 1100–1170 °C. However, this process does not lead to densification of the ceramics. Further, exo-trends followed by new melting endo-effects with peak temperatures at about 1300 °C are observed. Practically, the real sintering process starts at about 1200 °C and the densification can be related to the formation of melt, indicated by the second endo-effects.

Similar results were also obtained in other ceramics with huge amount of industrial waste.[9] It was demonstrated that the sintering in the range of first melting endo-effect is inhibited by re-crystallization processes and that the actual densification starts with the melting of the newly formed crystal phases.

The sintering behavior was also studied with samples heat-treated for 1 h at different temperatures in the range

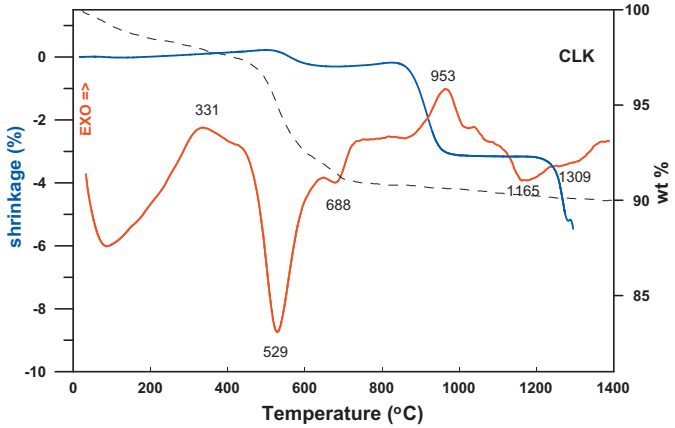

Fig. 2. DTA/TG and DIL curves of CLK composition.

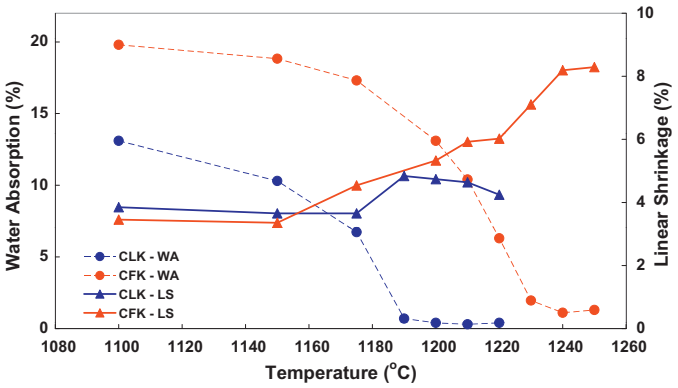

Fig. 3. Water absorption and linear shrinkage vs firing temperature.

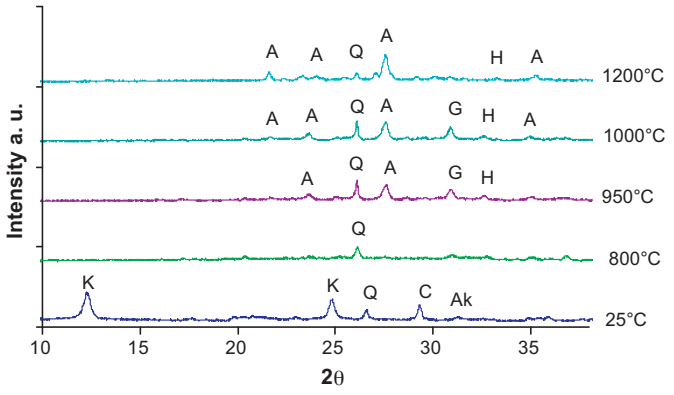

Fig. 5. XRD spectra of CFK composition at different temperatures. Q: quartz; K: kaolinite; C: calcite; H: hematite and A: anorthite.

1100–1250 °C. The initial porosities of these "green" samples were estimated about 37% and 33% for CFK and CLK, respectively. The results for the linear shrinkage (LS%) and water absorption (WA%) are summarized in Fig. 3, while information for the variations of open and closed porosities are reported in Fig. 4.

These results are in a good agreement with the dilatometric ones and highlight that both the intensive sintering begins after 1160–1180 °C and the shrinkage up to these temperatures (due to the kaolinite dehydration and the formation of alluminosilicates) is about 3%. The porosity in CFK at 1150 °C is higher than in the initial samples, confirming that the burning of organic residues and the decarbonization of limestone additionally increases the porosity. As a result, at similar values of the porosity the shrinkage in CFK is higher.

The densification of CLK composition occurs at low temperature. At 1200–1210 °C well sintered samples with WA% near zero and about 20% closed porosity are formed; at higher temperature starts overfiring. The optimal sintering range of CFK composition is 1230–1240 °C, where the WA% values are within 1.4–0.8% and the closed porosity is below 20%.

The phase transformations during heating and cooling were studied by XRD analysis, using a heating chamber. The results, obtained during heating are summarized in Figs. 5 and 6, while Figs. 7 and 8 report the spectra for CFK and CLK, respectively, gathered during cooling.

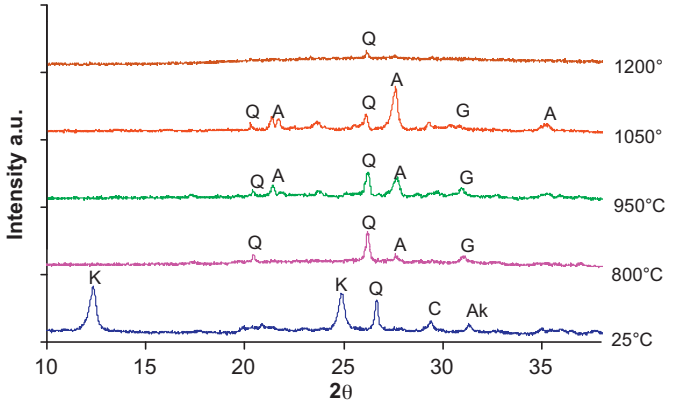

Fig. 6. XRD spectra of CLK composition at different temperatures. Q: quartz; K: kaolinite; C: calcite and A: anorthite.

The spectrum of initial CFK batch at room temperature (Fig. 5) corresponds to the main crystalline phases of used raw materials (i.e. kaolinite, quartz, calcite and akermanite). At 800 °C, after the deoxydrilation of kaolin and the decomposition of limestone, only quartz is present. At higher temperatures (950–1000 °C), in agreement with the DTA results which show a crystallization peak around 920 °C, formation of gehlenite ($Ca_2Al(AlSi)O_7$) [ICDD-01-087-0968] and anorthite ($CaAl_2Si_2O_8$) [ICDD-018-1202] is evidenced,

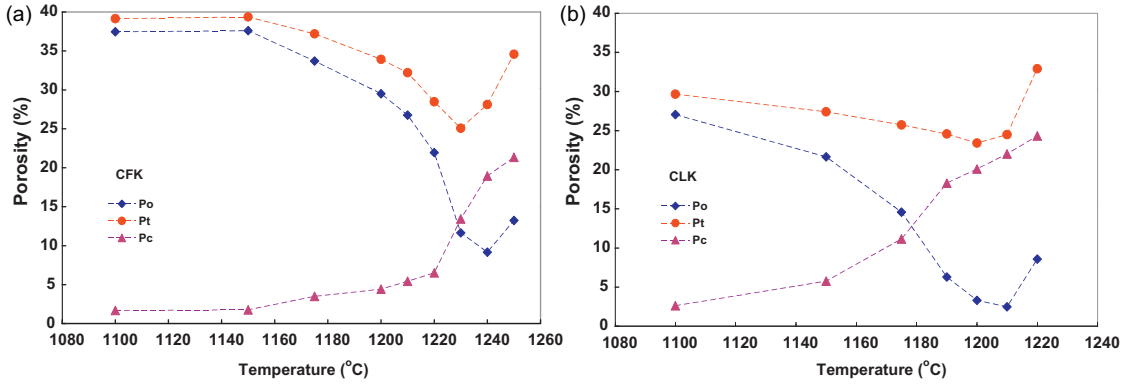

Fig. 4. P_O, P_C and P_T for CFK (a) and CLK (b) specimens vs firing temperature.

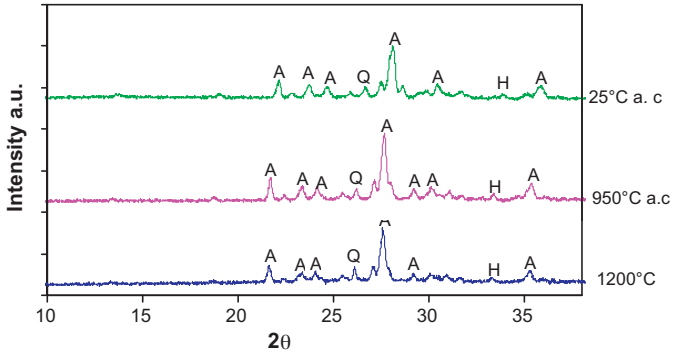

Fig. 7. XRD spectra of CFK composition after cooling (a.c.) at 950 and 25 °C compared to 1200 °C spectrum. Q: quartz, H: hematite and A: anorthite.

together with traces of hematite. At 1200 °C the gehlenite and quartz melt while the amount of anorthite phase increases (i.e. a re-crystallization process takes place). During cooling from 1200 to 950 °C (see Fig. 7) additional crystallization of anorthite occurs, resulting in ceramic products with high crystallinity.

The CLK composition shows similar behavior up to 1050 °C. In agreement with the higher content of silica and the lower of iron oxides in initial L composition, the spectra in Fig. 6 demonstrate large quartz amount and no formation of hematite. The re-crystallization process of gehlenite and quartz into anorthite is well highlighted at 1050 °C. At 1200 °C anorthite also melts and the corresponding spectrum shows only some undissolved quartz. The crystallization of anorthite during cooling and the high crystallinity of final CLK ceramics are well elucidated in Fig. 8.

3.2. Structure and properties of final ceramics

Surfaces and fractures of CLK and CFK ceramics, sintered at 1200 and 1230 °C, respectively, were observed by SEM (Figs. 9–11). The surfaces of both samples show good degree of densification with negligible open porosity. The sintered particles, as well as the open pores, are not smooth (as ones in the traditional ceramics) but are "rough" and polycrystalline. Fig. 9a

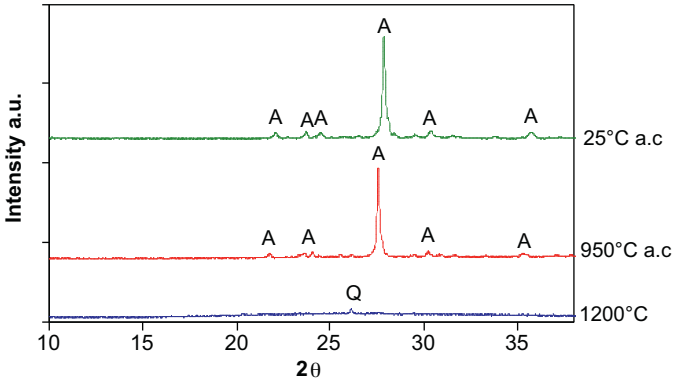

Fig. 8. XRD spectra of CLK composition after cooling (a.c.) at 950 and 25 °C compared to 1200 °C spectrum. Q: quartz and A: anorthite.

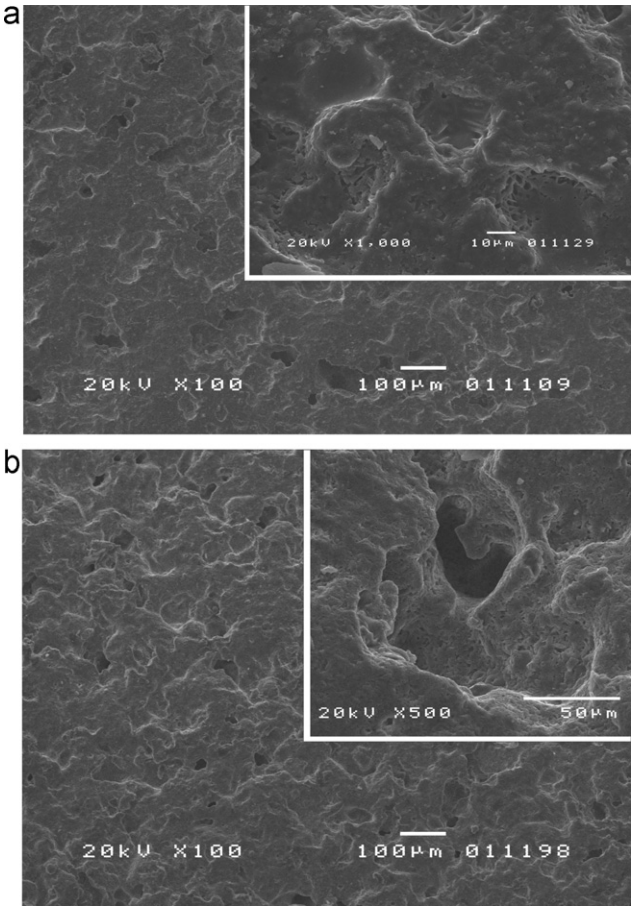

Fig. 9. SEM images of samples surface: (a) CLK fired at 1200 °C, 1 h; (b) CFK fired at 1230 °C, 1 h.

and b shows CLK and CFK surfaces at low magnification. The corresponding insets are details at higher magnification, showing the well sintered surface in CLK and a typical open pore, formed in CFK.

The CLK and CFK fractures are presented in Fig. 10a and b. In agreement with the pycnometric results, the comparison of images highlights a higher closed porosity in CLK ceramic. The joint of pores and the increasing of their size in CLK indicate the beginning of a coalescence process.

In both fractures, together with the semispherical big pores, additional tiny pores sized below 5–10 μm are observed. The formation of these pores might be related to the crystallization, carried out during sintering and cooling. The both kind of pores also show high crystallinity and are untypical for microstructures of the traditional ceramics. The inset in Fig. 10a presents a part of typical big close pore, while the inset in Fig. 10b shows a residual induced crystallization pore with size 4–6 μm.

The observed hexagonal crystals in the surface and in the pores of both samples were identified by EDS analysis as anorthite. Fig. 11 shows the typical morphology of these crystals (crystallization induced pore in CFK at 20,000 magnification).

On the basis of the thermal and sintering studies carried out on the laboratory samples, semi-industrial samples of the both

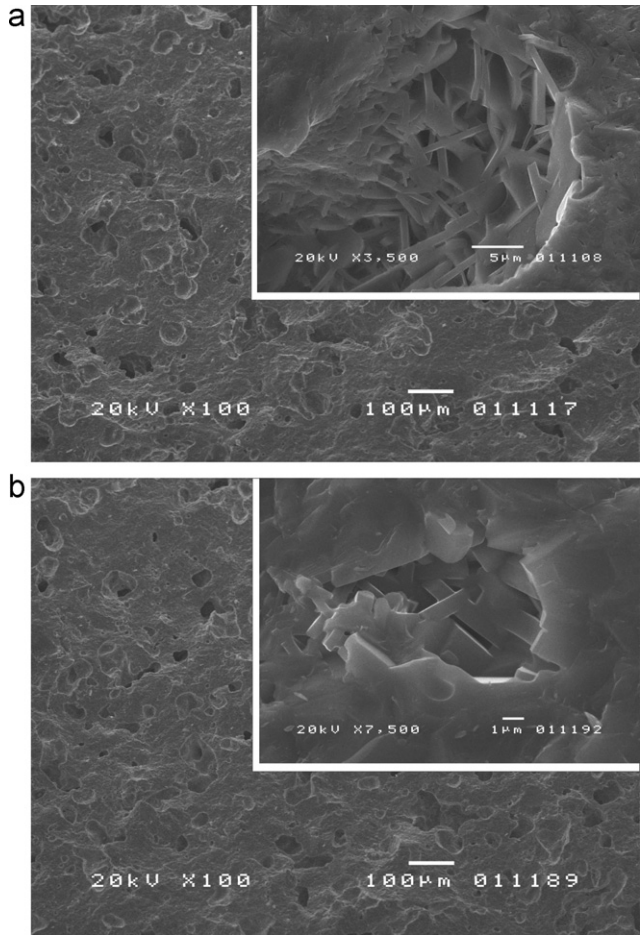

Fig. 10. SEM images of samples fracture: (a) CLK fired at 1200 °C, 1 h; (b) CFK fired at 1230 °C, 1 h.

compositions, fired at appropriate temperatures (at 1190 and 1210 °C for CLK and CFK, respectively) were obtained. Their technological properties were measured and the corresponding values are reported in Table 3.

Table 3
Technological properties: linear shrinkage (LS%), water absorption (WA%), measured densities, calculated porosities, bending strength (B.S.), Young's modulus (E), Mohs hardness and thermal expansion coefficients (α) for the semi-industrial fired samples CLK and CFK.

Properties	CFK	CLK
LS (%)	6.48	4.05
WA (%)	4.71	2.56
ρ_a (g/cm^3)	2.17	2.05
ρ_s (g/cm^3)	2.78	2.49
ρ_{as} (g/cm^3)	2.94	2.82
P_O (%)	20.6	15.7
P_C (%)	5.40	11.5
P_T (%)	26.0	27.3
B.S. (MPa)	47.67	42.09
E (GPa)	49.17	45.12
Mohs hardness	8	8
$\alpha \times 10^{-6}$ (°C^{-1})	6.14	6.22

The sintering parameters (LS% and WA%) and the porosity values are in agreement with ones from the laboratory studies and confirm that CFK composition shows higher values of LS% and WA% than CLK.

The distribution of the closed pores in the final samples was studied by mercury porosimetry. The method uses the non-wetting properties of mercury to gain information on the porous characteristics of solid materials: porosity, pore volume, pore size distribution, sample densities. This technique is extremely suitable for materials showing broad distributions of pore sizes, the pressure required to intrude mercury into the sample's pores is inversely proportional to the pores size.[31]

The results for CFK and CLK, corresponding to pore size distribution accompanied by Hg intrused volume data, are reported in Figs. 12 and 13. In CFK the main part of the pores have size between 10 and 30 μm, while in CLK larger pores (between 30 and 80 μm) are also presented. This detail confirms that the high closed porosity in CLK is mainly due to overfiring, which is related to the very narrow sintering interval.

Tiny pores (below 5–7 μm) observed by SEM are confirmed in both materials. This kind of porosity is untypical for the traditional ceramics[32] and can be related to the crystallization of anorthite during the sintering and cooling steps. The formation of similar crystallization induced porosity is studied in different sintered glass–ceramics.[33–35] Further, the creation of this additional fine porosity was also highlighted in new ceramic materials with high crystallinity.[9,36]

Notwithstanding that the semi-industrial specimens present 25-28% total porosity, the materials show mechanical properties higher than those prescribed in the EN ISO rule for high sintered commercial tiles (BIa group; WA ≤ 0.5%, B.S. > 35 MPa)[29,30] and good values of Young's modulus and Mohs hardness. These positive results can be related to the elevated presence of anorthite after firing and probably low amount of glassy residual phase. Finally, the mixtures show moderate thermal expansion coefficients between 20 and 400 °C (Table 3) suitable for avoiding the common glazes defects in firing (crazing, cracking).

Leaching tests were performed on the CFK and CLK semi-industrial samples, fired at 1210 and 1190 °C, respectively (Table 4). It has to be underlined that, at the moment the Italian environmental legislation does not contemplates an applicable test to check the leaching onto the end products such as ceramic tiles obtained by recycling different type of wastes, therefore it is reasonable apply a compliance test for leaching of granular waste materials and sludge (UNI 10802-UNI EN 12457-2).[27] In the absence of a reference specific table for the end product limits, values reported in Decree Ministerial 03/08/2005 (eluate limits for residues to landfill), have been chosen as reference. The results reported in Table 4, confirm that the thermal treatment at high temperatures (>1150 °C) permits to form a silicatic matrix able to incorporate and block the hazardous elements. Following the Italian regulation (in agreement with EU directives) about the waste landfilling, both the CFK and CLK materials can be classified as "not hazardous wastes". Moreover, it is important to note that the leaching values were obtained from tests carried

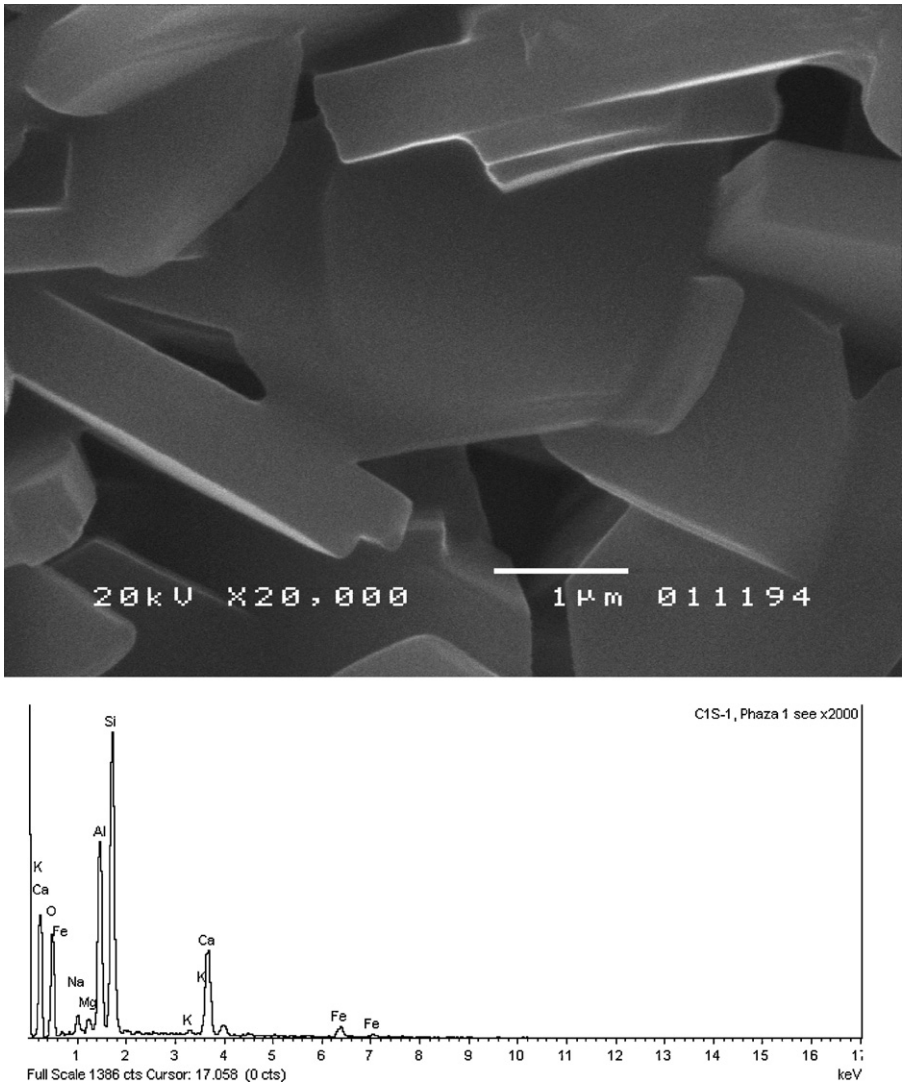

Fig. 11. Anorthite crystals, formed in crystallization induced pore (CFK) with corresponding EDS.

out on the granular (crashed) materials, thus more reactive than the compact samples. This means that on the bulk tile samples, the leaching values should be even lower. In any case, both the materials compared with the post-treated bottom ash (Table 4) show pH, conductivity and leaching values for all metals and anions lower than those reported for PTBA. In particular for Cl^{-}, SO_4^{2-} and Na^{+} a high inertization capability is shown. In this way, sintering is confirmed to be a valid method to fix alkali, anions and heavy metals, contained in this residue, into the ceramic matrix.

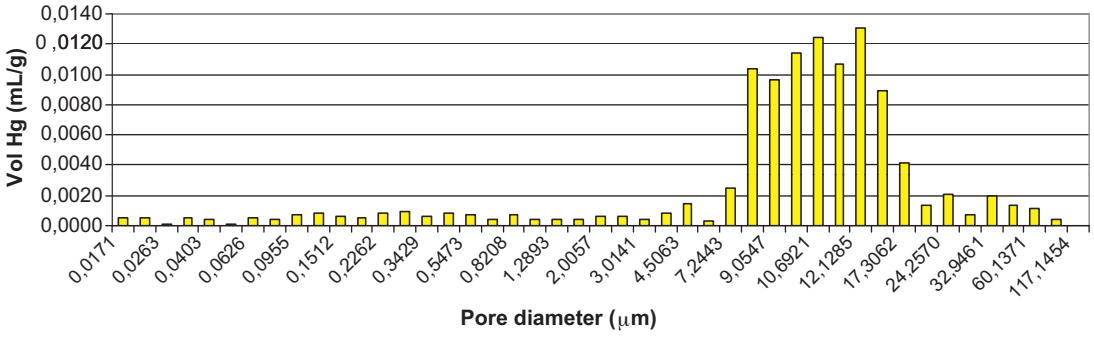

Fig. 12. Pore size distribution curve (Vol Hg vs pore dimensions) for CFK fired sample.

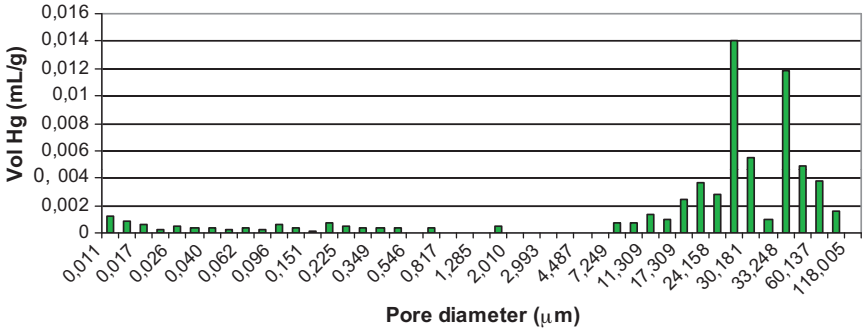

Fig. 13. Pore size distribution curve (Vol Hg vs pore dimensions) for CLK fired sample.

Table 4
Leaching test results of fired end products CFK and CLK compared to PTBA.

Metals/anions	PTBA elements released (mg/l)	CFK (1210 °C, 60′) elements released (mg/l)	CLK (1190 °C, 60′) elements released (mg/l)	Italian limit D.M. 03/08/2005 not hazardous waste (mg/l)
Cu	0.480	0.276	0.212	5.0
Zn	0.191	0.289	0.181	5.0
Ni	0.050	0.041	0.011	1.0
As	<0.05	<0.05	<0.05	0.2
Cd	0.008	0.00	0.00	0.02
Cr total	<0.001	<0.001	<0.001	1.0
Pb	0.530	0.142	0.042	1.0
Al	90.40	22.060	7.608	–
Fe	8.653	3.899	0.949	–
Na	151.00	8.364	4.579	–
Cl^-	200	12	9	1500
SO_4^{2-}	375	<0.2	5	2000
pH	10.68	8.10	7.16	5–12
S.C. (μS/cm)	1500	97.20	70.20	–

4. Conclusions

The presented study shows the feasibility to use high amounts of post-treated bottom ash as alternative raw material in clay-based ceramics compositions. The new ceramics were tailored to completely replace feldspar and quartz sand, and may be satisfactorily well-explained through SiO_2–Al_2O_3–CaO–Fe_2O_3 system with crystalline phases as anorthite, quartz and traces of hematite. This kind of residue permits to obtain building materials with technological properties similar to commercial ones without use traditional fluxes and inert materials. According to the UNI EN ISO standards the obtained tile samples could be classified into BIb and BIIa groups (WA% values within 2–5%) but having mechanical properties higher than those prescribed for high sintered materials (B.S. >35 MPa for BIa group).

Finally, significant environmental benefits are attained: (a) avoided storage of bottom ash and minimization of the natural resources consumption; (b) obtainment of new ceramics with a good level of environmental safety by ceramic firing; (c) avoided pre-washing process, necessary for the utilization of PTBA for example in cement for which strong Cl^- restriction is required.

Acknowledgements

The work was supported by Project DID-02/40 (Bulgarian Ministry of Science and Education) and the Programme for Scientific and Cultural Collaboration between Modena and Reggio Emilia University and Bulgarian Academy of Sciences for Italian researches mobility.

References

1. Gennaro R, Cappelletti P, Cerri G, Gennaro M, Dondi M, Guarini G, et al. Influence of zeolites on the sintering and technological properties of porcelain stoneware tiles. *J Eur Ceram Soc* 2003;**23**:2237–45.
2. Carbonchi G, Dondi M, Morandi N, Tateo F. Possible use of altered volcanic ash in ceramic tile production. *Ind Ceram* 1999;**19**:67–74.
3. Ergul S, Akyildiz M, Karamanov A. Ceramic material from basaltic tuffs. *Ind Ceram* 2007;**37**:75–80.
4. Salem A, Jazayeri SH, Rastelli E, Timellini G. Dilatometric study of shrinkage during sintering process for porcelain stoneware body in presence of nepheline syenite. *J Mater Process Technol* 2009;**209**:1240–6.
5. Tucci A, Esposito L, Rastelli E, Palmonari C, Rambaldi E. Use of soda-lime scrap-glass as a fluxing agent in a porcelain stoneware tile mix. *J Eur Ceram Soc* 2004;**24**:83–92.
6. Andreola F, Barbieri L, Karamanova E, Lancellotti I, Pelino M. Recycling of CRT panel glass as fluxing agent in the porcelain stoneware tile production. *Ceram Int* 2008;**34**(5):1289–95.
7. Torres P, Fernandes HR, Agathopoulos S, Tulyaganov DU, Ferreira JMF. Incorporation of granite cutting sludge in industrial porcelain tile formulations. *J Eur Ceram Soc* 2004;**24**:3177–85.
8. Andreola F, Barbieri L, Bondioli F, Ferrari AM, Lancellotti I, Miselli P. Recycling screen glass into new traditional ceramic materials. *Int J Appl Ceram Technol* 2010;**7**(6):909–17.
9. Karamanova E, Avdeev G, Karamanov A. Ceramics from blast furnace slag, kaolin and quartz. *J Eur Ceramic Soc* 2011;**31**(6):989–98.

10. Barbieri L, Corradi A, Lancellotti I, Manfredini T. Use of municipal incinerator bottom ash as sintering promoter in industrial ceramics. *Waste Manage* 2002;**22**:859–63.
11. Dana K, Das SK. Partial substitution of feldspar by B.F. slag in triaxial porcelain: phase and microstructural evolution. *J Eur Ceram Soc* 2004;**24**:3833–9.
12. Zanelli C, Baldi G, Dondi M, Ercolani G, Guarini G, Raimondo M. Glass ceramic frits for porcelain stoneware bodies: effects on sintering, phase composition and technological properties. *Ceram Int* 2008;**34**(3): 455–65.
13. ISPRA - Istituto Superiore per la Protezione e la Ricerca Ambientale. Waste Report; 2008. http://www.apat.gov.it/site/it-IT/APAT/Pubblicazioni/Rapporto_Rifiuti.
14. European Commission, Directorate-General Jrc, Joint Research Centre, Institute for Prospective Technological Studies (Seville), Technologies for Sustainable Development European IPPC Bureau, Integrated Pollution Prevention and Control Draft Reference Document on the Best Available Techniques for Waste Incineration, Draft March; 2004.
15. Lapa N, Barbosa R, Morais J, Mendes B, Mehu J, Santos Oliveira JF. Ecotoxicological assessment of leachates from MSWI bottom ashes. *Waste Manage* 2002;**22**:583–93.
16. ENEA, Italian National Agency for New Technology, Energy and the Environment, Technical report on energy from municipal waste in Italy; 2009. http://www.enea.it/produzione_scientiica/pdf_volumi/V2009_06Rapporto_RecuperoRifiuti.pdf.
17. Kasuriya S, Jiermsiriliers S, Thavorniti P. Effect of MSW incineration bottom ash in clay based ceramics. *Proc Mater Science Forum* 2008;**569**:205–8.
18. Ferraris M, Salvo M, Ventrella A, Buzzi L, Veglia M. Use of vitrified MSWI bottom ashes for concrete production. *Waste Manage* 2009;**29**:1041–7.
19. Andreola F, Barbieri L, Lancelloti I, Pozzi P. Industrial waste recycling in bricks manufacture. 1st part. *Materiales de Costrucciòn* 2005;**55**(280): 5–16.
20. Rambaldi E, Esposito L, Andreola F, Barbieri L, Lancellotti I, Vassura I. The recycling of MSWI bottom ash in silicate based ceramic. *Ceram Int* 2010;**36**:2469–76.
21. EN 14411, Ceramic Tile-Definitions, Classification, Characteristics and Marking; 2006.
22. Almeida MIA, Amaral MR, Sousa Correira AM, Fonseca Almeida M. Ceramic building materials: an alternative in disposal of sewage sludge. *Key Eng Mater* 1997:2280–4, 132–136.
23. Perez JA, Terradas R, Manent MR, Seijas M, Martinez M. Inertization of industrial wastes in ceramic materials. *Ind Ceram* 1996;**16**(1):7–10.
24. Couto DMS, Silva RF, Castro F, Labrincha JA. Inertization of metallurgical sludges in clay-based ceramics. In: Gomes CS, editor. *Proceedings of the 2nd Mediterranean clay meeting, vol. 2*. 1998. p. 214–9.
25. Heritage K, Frisby C, Wolfender M. Impulse excitation technique for dynamic flexural measurements at moderate temperature. *Rev Sci Instrum* 1988;**59**:973–4.
26. http://www.icdd.com/.
27. EN 12457-2. Characterization of waste. Leaching compliance test for leaching of granular waste materials and sludge; 2002.
28. Donald IW. *Waste Immobiliztion in Glass and Ceramics Based Hosts, Vitrification of Nonradioactive Toxic and Hazardous Wastes*. Wiley; 2010.
29. Manfredini T, Pellacani GC, Romagnoli M. Porcelain stoneware tiles. *Am Ceram Soc Bull* 1995;**74**(5):76–9.
30. U NI EN 14411(ISO 13006). Single firing technical characteristics; 2003.
31. http://www.azom.com/article.aspx?ArticleID=3227;http://www.micromeritics.com/Repository/Files/Porosimetry_brochure.pdf.
32. Dondi M, Ercolani G, Guarini G, Melandri C, Raimondo M, Rocha E, et al. The role of surface microstructure on the resistance to stains of porcelain stoneware tiles. *J Eur Ceram Soc* 2005;**25**:357–65.
33. Karamanov A, Pelino M. Induced crystallization porosity and properties of sintered diopside and wollastonite glass–ceramics. *J Eur Cer Soc* 2008;**28**:555–62.
34. Schabbach L, Andreola F, Karamanova E, Lancellotti I, Karamanov A, Barbieri L. Integrated approach to establish the sinter-crystallisation ability of glasses from secondary raw material. *J Non-Crystalline Solids* 2011;**357**:10–7.
35. Abyzov AS, Schmelzer JWP, Fokin V.M. Theory of pore formation in glass under tensile stress: generalized Gibbs approach. *J Non-Crystalline Solids* 2011;**357**(19-20):3474–9.
36. Karamanov A, Arrizza L, Ergul S. Sintered material from alkaline basaltic tuffs. *J Eur Ceram Soc* 2009;**29**:595–601.